1996MNRAS.282..157B

Mon. Not. R. Astron. Soc. **282,** 157–166 (1996)

Shadowing of the 0.25-keV extragalactic X-ray background by the disc of NGC 55

C. R. Barber, T. P. Roberts and R. S. Warwick

Department of Physics and Astronomy, University of Leicester, Leicester LE1 7RH

Accepted 1996 April 11. Received 1996 April 4; in original form 1996 February 5

ABSTRACT

ROSAT observations are used to search for a shadow in the 0.25-keV X-ray background cast by the disc of the nearby spiral galaxy NGC 55. Several factors, including the close to edge-on aspect of this galaxy, its extensive H I disc and its location in a direction of relatively low Galactic foreground column density, make NGC 55 an excellent target in which to search for such effects. The *ROSAT* PSPC image shows a clear deficit of 0.25-keV counts coincident with the outer disc of NGC 55. From the depth of the shadow we obtain an estimate of the total extragalactic background signal at 0.25 keV of 29.4 ± 7.2 keV cm^{-2} s^{-1} sr^{-1} keV^{-1}. We compare this measurement with other recent estimates of the 0.25-keV background intensity, and briefly discuss the implications of the result in the context of the source populations which may produce the X-ray background radiation.

Key words: diffuse radiation – X-rays: general.

1 INTRODUCTION

Although more than 30 years have passed since the discovery of the cosmic X-ray background (XRB) (Giacconi et al. 1962), the origin of this phenomenon is still keenly debated (see Fabian & Barcons 1992 for a review). The observed isotropy of the background at energies above 3 keV establishes an extragalactic origin for this hard radiation. Current interest centres on identifying the types of discrete X-ray source which may contribute significantly to this background, with the constraint that the integrated spectral properties of the dominant source population (or populations) must match the observed 40-keV thermal-bremsstrahlung spectral form of the hard XRB (Marshall et al. 1980). For example, it has been suggested recently that an evolving population of galaxies having a hidden active nucleus may play a significant role in the synthesis of the XRB spectrum on the basis of the intrinsically hard X-ray spectra of such sources (Madau, Ghisellini & Fabian 1994; Comastri et al. 1995).

In contrast to the situation above 3 keV, at lower energies the XRB exhibits a spatial distribution which is clearly non-isotropic (see the review by McCammon & Sanders 1990). This suggests the emergence of one or more local components of the background with a relatively soft spectral form. In the 0.5–1.0 keV band the average XRB intensity is a factor ~ 2 above a simple extrapolation of the power-law form (with an energy index of 0.4) which quite accurately characterizes the XRB spectrum in the 3–10 keV range (Marshall et al. 1980). The excess emission is undoubtedly of Galactic origin and must include a contribution from Galactic dM stars (Schmitt & Snowden 1990) in addition to that from hot ($T \approx 10^{6.5}$ K) optically thin plasma (Nousek et al. 1982). In this band much of the observed spatial structure in the XRB can be identified with particular features in our Galaxy (e.g., Loop I, the Vela SNR and the Cygnus Superbubble). In the adjacent 0.1–0.4 keV band the average XRB intensity exceeds the extrapolated hard power law by a factor ≥ 3, with the Galactic poles being generally brighter than the Galactic plane. There is good evidence that much of the emission is due to a $T \approx 10^6$ K plasma situated within the local low-density cavity in the interstellar medium (ISM) (Snowden et al. 1990). However, based largely on *ROSAT* observations of shadows cast by discrete clouds in the Galactic ISM, it has been possible, albeit for a limited number of directions, to separate the very local soft X-ray emission from that arising in a much more extensive Galactic component, which in some cases appears to extend into the Galactic halo (Burrows & Mendenhall 1991; Snowden et al. 1991; Wang & Yu 1995).

It has proved extremely difficult to untangle the extragalactic XRB intensity in the spectral range below ~ 2 keV from the Galactic signal. For example, there is currently considerable uncertainty as to the normalization and spec-

© 1996 RAS

© Royal Astronomical Society • Provided by the NASA Astrophysics Data System

1996MNRAS.282..157B

tral slope of the extragalactic XRB at 1 keV (see Hasinger 1992 and Gendreau et al. 1995). The problem is even more acute in the 0.1–0.4 keV band (in this paper we generally refer to this soft X-ray band as the 0.25-keV band). In this band the extragalactic signal, after allowing for significant absorption by interstellar material along the line of sight,[1] is all but swamped by the Galactic emission. Undoubtedly the best way of sorting out the contributions in the 0.25-keV band of the emission from the local bubble, from more distant Galactic components, and also of extragalactic origin is through shadowing experiments. In particular, if the shadow of an extragalactic object, say the disc of a spiral galaxy, could be detected superimposed on the extragalactic background then, provided the characteristics of the absorbing screen are reasonably well determined, the depth of the shadow provides a direct measurement of the intensity of extragalactic background. This approach is employed in the present paper, leading to a determination of extragalactic XRB intensity at 0.25 keV.

In a previous paper (Barber & Warwick 1994, hereafter BW94) we have shown that the *ROSAT* Position Sensitive Proportional Counter (PSPC) affords an excellent opportunity to search for the shadowing effects of galactic discs on the extragalactic soft XRB. The constraints on possible shadowing targets are rigorous. The spiral galaxy must not itself be a bright source of soft X-rays, its H I distribution must have been mapped at sufficient angular resolution to match the X-ray data, and the foreground H I column density (in our own Galaxy) must be low. Further, the practical limitations of the *ROSAT* PSPC and current limits on the extragalactic intensity require that the shadowed region must subtend a significant solid angle (i.e., many tens of square arcmin).

In this paper we report the analysis of a *ROSAT* PSPC observation of the spiral galaxy NGC 55, which is a member of the nearby Sculptor group of galaxies. NGC 55 is classified as SB(s)m (de Vaucouleurs, de Vaucouleurs & Corwin 1976) and has a close to edge-on configuration. Its extensive H I disc, its location in a direction of relatively low Galactic foreground column density, and its modest X-ray luminosity (see below) make NGC 55 an excellent target for a shadowing study.

2 THE *ROSAT* PSPC OBSERVATION AND DATA ANALYSIS

A *ROSAT* PSPC observation of NGC 55 was performed during the period 1991 November 22–24 and gave a total exposure time of 18 993 s. The initial data selection involved the exclusion of periods during which the on-board charged-particle master-vetoing rate exceeded a threshold of 170 count s^{-1} (allowing the residual charged-particle contribution to be modelled – Snowden et al. 1992; Plucinsky et al. 1993). This constraint leads to a 4.7 per cent loss of data. Fig. 1 shows the central 40×40 arcmin^2 region of the 0.25-keV *ROSAT* PSPC image (corresponding to PI channels 11–41) obtained by binning the data into 15×15 arcsec^2 pixels and convolving the resulting image with a two-dimensional Gaussian with full width at half-maximum (FWHM) of 1.5 arcmin. In order to reduce the effects of the telescope vignetting and the possibility of foreground XRB variations, we consider only the central 18-arcmin radius region of the PSPC field of view in the present analysis.

We proceed to remove instrumental effects and non-cosmic contamination from the 0.25-keV band PSPC data by using the scheme of Snowden et al. (1994). This accounts for contamination by solar-scattered X-rays, non-vetoed high-energy charged particles and, as far as is possible, long-term background enhancements. It also corrects for the telescope vignetting function, obscuration of some parts of the detector by window support structures, and the PSPC afterpulsing phenomenon. It should be noted that the process is insensitive to a general baseline shift in the data, so the intensity observed is an upper limit to the true cosmic intensity. The complete analysis of a PSPC observation considers the data in seven 'R' bands (R1L to R7) which take nearly full advantage of the PSPC energy resolution. However, for the present work we consider the count rates measured in the combined R1L and R2 band (which extends over the PI channel range of the 0.1–0.4 keV band). Table 1 details the contribution of the various processes in the combined R1L/R2 band as estimated using the Snowden technique. These identified 'contaminants' have been projected, with the relevant spatial distributions, into a single count space map, which is then subtracted from the corresponding rate R1L/R2 map. The detector efficiency map is projected on to the sky with the same orientation and wobble as the observation itself, and the resulting exposure map (which accounts for telescopic vignetting and obscuration) is then used to flat-field the contamination-free data map, yielding a 'clean' 0.25-keV image. Finally, as a check of the validity of the above process, we have subtracted the combined contribution of the contaminants in each band from the observed data as a function of time. The resulting light curves exhibit considerable stability, implying that we have identified all of the sources of contamination which are present (except for a possible baseline shift, as noted earlier).

The central 18-arcmin radius region of the 'clean' 0.25-keV image was finally rebinned into a total of 256 pixels of size 2×2 arcmin^2. The average intensity was $\sim 690 \times 10^{-6}$ count s^{-1} arcmin^{-2}, with a typical statistical error of ~ 15 per cent.

Next, we attempt to minimize the effect of the bright discrete sources evident in Fig. 1. As a preliminary step we employed the point-source search algorithm PSS (which is part of the UK Starlink ASTERIX software package; Allen 1992) to search for point-like enhancements above the local background in the original (15×15 arcsec^2 pixel) 0.25-keV image. PSS found six such sources with a significance of more than 4.5σ within the central 18-arcmin radius field; details of these sources are given in Table 2. Assuming a power-law source spectrum with an energy index $\alpha = 1$, and absorption by a Galactic column density $N_H = 1.55 \times 10^{20}$ cm^{-2} (Stark et al. 1992), the minimum 0.25-keV count rate of 2.0×10^{-3} count s^{-1} corresponds to a 0.5–2.0 keV band count rate of 2.1×10^{-3} count s^{-1} and a flux of 2.6×10^{-14} erg cm^{-2} s^{-1} (0.5–2.0 keV). In the present paper we use this 'standard' spectral conversion on a number of occasions. The influence of the discrete soft sources identified in Table 2 was removed using the scheme adopted by BW94. Thus 2×2 arcmin^2 pixels in the background map were excluded if

[1] At 0.25 keV an optical depth of unity corresponds to a column density of cold solar-abundance gas of only $N_H \sim 10^{20}$ cm^{-2}.

© Royal Astronomical Society • Provided by the NASA Astrophysics Data System

1996MNRAS.282..157B

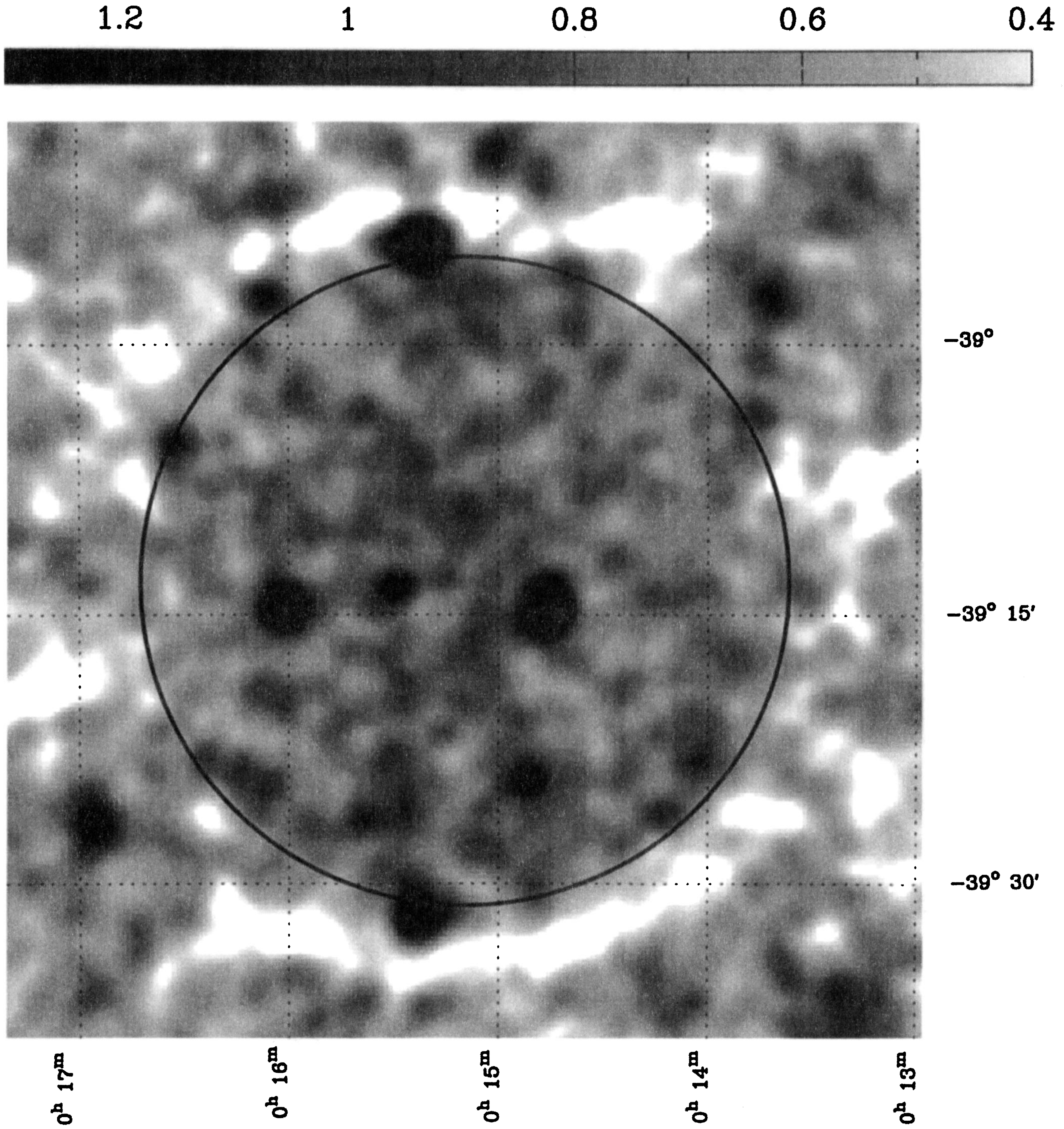

Figure 1. The central region of the 0.25-keV *ROSAT* PSPC image. The ring is drawn at a radius of 18 arcmin. The data have been smoothed with a two-dimensional Gaussian with a FWHM of 1.5 arcmin but not (at this stage) exposure- or background-corrected. The grey-scale has units of count pixel^{-1}.

the pixel centres were within a radius of 3 arcmin of a discrete source containing greater than 100 counts in the 0.25-keV image. Similarly, the exclusion radius was 1.5 arcmin for sources with less than 100 soft counts. On this basis, 24 of the 2×2 arcmin^2 pixels were excluded from the analysis.

As a further check on the effect of bright discrete sources, we have analysed the 0.5–2.0 keV *ROSAT* image. This resulted in 43 source detections at a significance greater than 4.5σ (within the central 18-arcmin radius field), six of which have count rates greater than 2.1×10^{-3} count s^{-1} (the equivalent 0.5–2.0 keV count rate threshold noted

© Royal Astronomical Society • Provided by the NASA Astrophysics Data System

1996MNRAS.282..157B

Table 1. Contribution of contaminants in the 0.25-keV PSPC image.

Contaminant	Raw Counts	Percentage of total counts
Long term enhancement	7007	7.4
Detector afterpulses	1180	1.2
Solar contamination	1388	1.5
Residual Charged Particles	340	0.4

Table 2. Bright point sources detected in the *ROSAT* PSPC images.

RA (2000)	Dec(2000)	0.1–0.4 keV count s^{-1}	0.5–2.0 keV count s^{-1}	Coincident with NGC55?	Comments
soft sources					
00 14 02.7	-39 23 06	2.5×10^{-3}	2.9×10^{-3}	N	
00 14 45.8	-39 14 34	1.6×10^{-2}	2.7×10^{-2}	Y	Foreground Star
00 14 51.5	-39 24 17	3.4×10^{-3}	1.9×10^{-3}	N	
00 15 29.0	-39 13 27	3.9×10^{-3}	1.7×10^{-1}	Y	
00 15 38.2	-39 26 30	2.0×10^{-3}	1.1×10^{-3}	N	
00 16 01.3	-39 14 40	9.5×10^{-3}	-	Y	Supersoft Source
hard sources					
00 14 20.1	-39 11 16	-	6.9×10^{-3}	Y	
00 14 37.1	-38 59 14	-	2.6×10^{-3}	N	
00 14 52.4	-39 10 50	-	2.6×10^{-2}	Y	Bar Complex

above). Three of these detections, the 'hard sources' in Table 2, have no soft-band counterpart and therefore exhibit significantly harder spectra than our standard spectral form. Although undetected in the soft band, we have chosen to remove the possible contribution of these three sources by treating them as <100 count soft-band detections. This leads to the loss of a further five pixels. Fig. 2 shows a grey-scale representation of the remaining array of 0.25-keV intensity measurements.

3 EVIDENCE FOR A SHADOW

To determine the expected depth of a shadowed extragalactic signal, we use the H I map of Puche, Carigan & Wainscoat (1991). The resolution of the H I map, $\sim 80 \times 80$ arcsec^2, facilitates comparison with the 2×2 arcmin^2 pixel size of the X-ray data. Fig. 2 shows the H I contours from Puche et al. (1991) overlaid on to the 0.25-keV background intensity measurements. A total of 69 pixels overlap with the measured H I distribution of NGC 55 (i.e., the pixel centre is encompassed by the minimum contour in Fig. 2), leaving the remaining 158 pixels as a 'control' sample.

An important assumption of shadowing experiments is that the region casting the shadow is not sufficiently X-ray-bright as to compromise the absorption measurements. In order to investigate the possible masking of shadowing effects by soft *diffuse* emission associated with NGC 55, we have divided the 69 'on-source' pixels into two subsamples. Thus pixels from regions within a 7.5-arcmin radius of the centre of NGC 55 (taken to be the centroid of the disc component; see Hummel, Dettmar & Wielebinski 1986) form an 'inner-disc' sample, and those outside of this radius give an 'outer-disc' sample. The frequency distributions of the pixel intensities in the control and on-source samples are shown in Fig. 3, and the corresponding mean and standard error value are given in Table 3. These data suggest the presence of a shadow cast by the outer-disc regions of NGC 55, but with no counterpart for the inner-disc region.

In Fig. 4 we plot the average background intensities measured in both the inner- and the outer-disc regions of NGC 55 for three ranges of the H I column density within the NGC 55 disc. For the outer-disc data the observed profile is fully consistent, within the limits of the statistics, with the presence of a shadowing effect. However, there is no evidence for a similar feature for the inner-disc region. The most likely interpretation of the latter result is in terms of in-filling of the putative shadow by either diffuse emission or unresolved point sources located within ~ 3.5 kpc of the centre of NGC 55 (assuming that the galaxy is at a distance of 1.6 Mpc – see Puche & Carignan 1988). We find that if the radius of the inner-disc region is decreased, the apparent enhancement in the 0.25-keV emission of the inner disc increases somewhat, whereas the converse is true if this radius is increased, consistent with the excess emission having a central concentration. Based on the level of outer-disc emission for $N_H > 10^{21}$ cm^{-2} (Fig. 4), the peak surface brightness of the in-filling emission in the inner-disc

© Royal Astronomical Society • Provided by the NASA Astrophysics Data System

1996MNRAS.282..157B

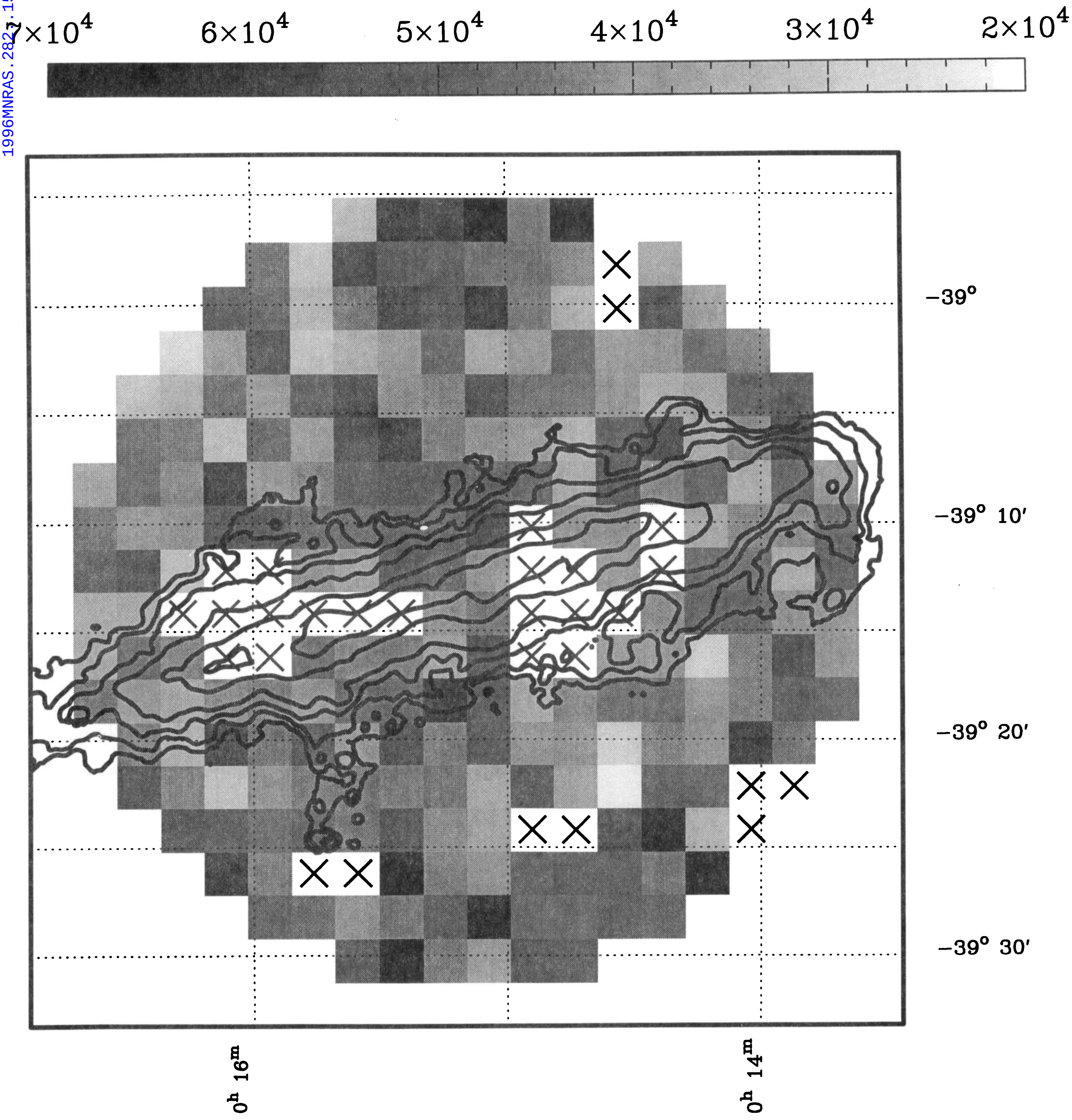

Figure 2. The central region of the 'clean' 0.25-keV *ROSAT* PSPC image with the background measurements binned into pixels of 2 × 2 arcmin^2. Those pixels affected by discrete sources are set to zero (and for clarity marked by a cross). The H I measurements are derived from the map of Puche et al. (1991), with the contour levels corresponding to $N_H = 0.5$, 2, 5, 10, 30 and 60 × 10^{20} cm^{-2}. The grey-scale has units of 1/64 × 10^{-6} count s^{-1} arcmin^{-2}.

region is probably in the range ~(50–70) × 10^{-6} count s^{-1} arcmin^{-2}. (We can exclude a very much higher value, since the lowest N_H bin for the inner disc in Fig. 4 does not show a prominent excess above the control level.) If this emission is thermal with a temperature of ~10^6 K, subject to only Galactic foreground absorption and extends over an area of ~50 arcmin^2, then the corresponding X-ray luminosity in the 0.25-keV band is ~10^{37} erg s^{-1}. Interestingly, of the point sources listed in Table 2, only the supersoft source, with $L_X \approx 4 \times 10^{37}$ erg s^{-1}, has a higher apparent 0.25-keV

© Royal Astronomical Society • Provided by the NASA Astrophysics Data System

1996MNRAS.282..157B

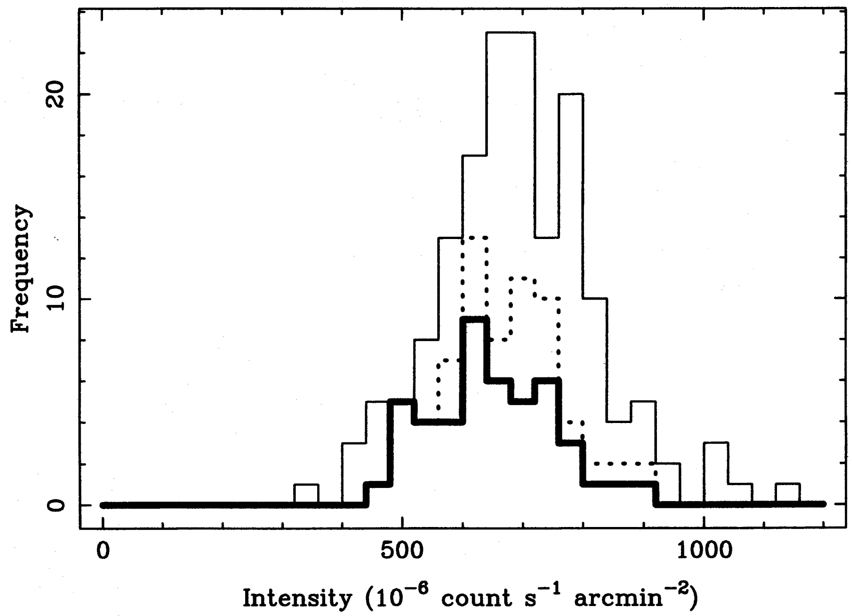

Figure 3. Histograms of the count rates measured in the 0.25-keV *ROSAT* PSPC image for the control sample (thin line), the outer-disc sample (thick line) and the inner- plus outer-disc sample (dashed line).

Table 3. The mean 0.25-keV count rates for the three regions.

Region	No. pixels	Mean count rate (count s^{-1} $arcmin^{-2}$)
Control	158	$690 \pm 11 \times 10^{-6}$
Inner disk	23	$691 \pm 18 \times 10^{-6}$
Outer disk	46	$643 \pm 15 \times 10^{-6}$

band luminosity. Thus NGC 55 is far from being a luminous source of soft X-rays.

However, an important question which still needs to be addressed is whether the shadow of the outer disc might also be partially masked by unresolved 0.25-keV emission from NGC 55. In this context it is useful to make a comparison with the face-on Sc supergiant spiral M101. In a recent study, Snowden & Pietsch (1995) have shown that this galaxy is a bright and extended soft X-ray source, and have

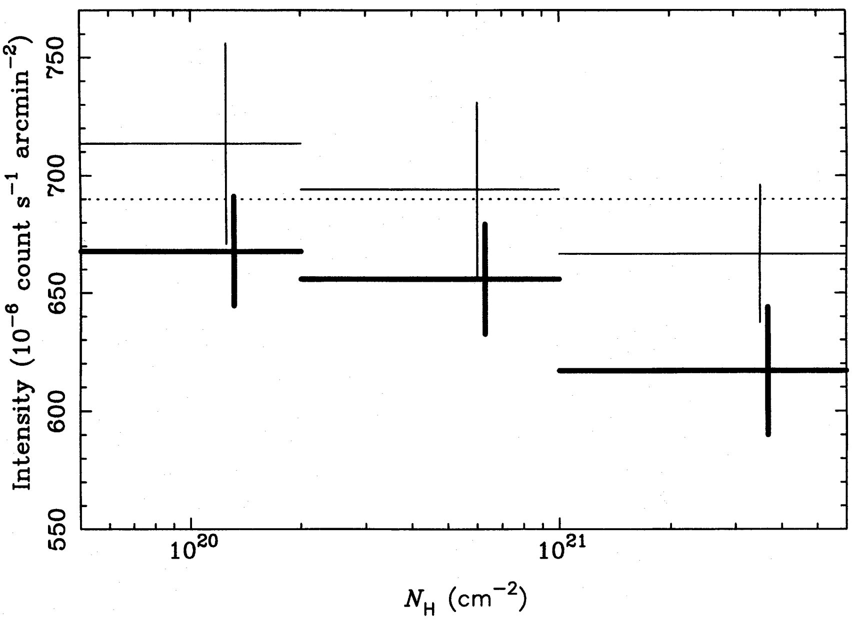

Figure 4. The average 0.25-keV count rate for the inner-disc sample (thin line) and the outer-disc sample (thick line) plotted for three ranges of N_H. The dotted line corresponds to the average surface brightness measured in the control region.

© Royal Astronomical Society • Provided by the NASA Astrophysics Data System

1996MNRAS.282..157B

derived the radial profile of its 0.25-keV emission over an angular scale of 0–20 arcmin. Although the distance of M101 is a factor ~ 4.5 greater than that of NGC 55, the corrected D_{25} diameter of the two galaxies is almost the same (23.8 and 24.2 arcmin for M101 and NGC 55 respectively – Tully 1988). From the 0.25-keV radial profile of M101, the ratio of the average (area-weighted) surface brightness within a radius of 7.5 arcmin to that in the annulus between radii of 7.5–17.5 arcmin is ~ 4. Although in going from a face-on to an edge-on aspect a number of unknown geometrical (e.g., emission scaleheight) and absorption corrections will apply, this does support the possibility of a significant fall-off in the intensity of diffuse/unresolved component between the inner- and outer-disc regions in NGC 55. The fact that the lowest $N_{\rm H}$ bin for the outer disc in Fig. 4 lies below the control level is also consistent with the hypothesis that any masking of the shadow in this region of the disc is slight. In the present paper we take the view that the depth of shadow observed in the outer-disc region of NGC 55 (beyond a radius of 7.5 arcmin) provides an effective measure of the intensity of the 0.25-keV extragalactic background rather than simply giving a lower limit value.

4 THE 0.25-keV EXTRAGALACTIC XRB INTENSITY

We have applied a statistical weighting technique similar to that described in BW94 to the 46 intensity measurements for the outer-disc region of NGC 55, in order to obtain a best estimate of the 0.25-keV extragalactic background intensity, $C_{\rm ext}$. Specifically, $C_{\rm ext}$ is the extragalactic XRB intensity, corrected for all line-of-sight absorption, *after* excluding point sources to a particular 0.25-keV sensitivity threshold. One problem is that this threshold (when expressed in terms of the intrinsic source flux in, say, the 0.5–2 keV band) actually varies between the control region, where the absorption is due only to the foreground Galactic H I, and the on-source regions, where there is significant additional absorption due to the H I in the disc of NGC 55. In effect, the source-exclusion process is less effective in removing sources for the on-source regions, since the extra absorption reduces the 0.25-keV count rate of discrete sources behind NGC 55. In Appendix A the method of BW94 is reformulated to account for this varying threshold. The result is a correction term which should be incorporated in equation (4) of BW94; however, in practice this correction amounts to only a ~ 5 per cent effect, which is small compared with the statistical errors.

Using the method described in Appendix A, we derive a weighted mean value $C_{\rm ext} = (228 \pm 90) \times 10^{-6}$ count s^{-1} arcmin^{-2}. This is a 2.5σ positive detection of the *unresolved* extragalactic background. Allowing for a transmission of only 29 per cent through the foreground Galactic H I column ($N_{\rm H} = 1.55 \times 10^{20}$ cm^{-2}), the *observed* extragalactic signal is thus 66×10^{-6} count s^{-1} arcmin^{-2}, or ~ 10 per cent of the total observed 0.25-keV band background signal. Assuming that the spectrum of the extragalactic emission can be reasonably represented by a power law of energy index $\alpha = 1$ (the in-band conversion is not very sensitive to the assumed spectral form), the derived count rate corresponds to an intensity at 0.25 keV of 18.2 ± 7.2 keV cm^{-2} s^{-1} sr^{-1} keV^{-1}. It is important to recall that this 0.25-keV background intensity is obtained after removing discrete sources with a 0.25-keV count rate greater than 2×10^{-3} count s^{-1}, which based on our 'standard' spectral model converts to a 0.5–2.0 keV flux threshold of 2.6×10^{-14} erg cm^{-2} s^{-1}. We use the 0.5–2.0 keV source counts of Hasinger et al. (1993) to determine the combined flux of sources brighter than this limit as 2.80 keV cm^{-2} s^{-1} sr^{-1} keV^{-1} at 1 keV, or 11.2 keV cm^{-2} s^{-1} sr^{-1} keV^{-1} at 0.25 keV. Thus the *total* extragalactic background intensity at 0.25 keV becomes 29.4 ± 7.2 keV cm^{-2} s^{-1} sr^{-1} keV^{-1}.

The derived 0.25-keV XRB intensity is rather sensitive to the assumed value for the transmission through the foreground Galactic absorption, and thus it is important to consider the possible impact of the uncertainty in this parameter. In particular, the use of the Galactic H I column density[2] will lead to an underestimate of the true line-of-sight absorption if, in addition to neutral gas, there is a substantial molecular or ionized component present (e.g. McCammon & Sanders 1990; BW94). The presence of such additional absorbing material would lead to an underestimate of the intensity of the 0.25-keV XRB intensity.

To check for the presence of molecular hydrogen, we have used the list of Desert, Bazell & Boulanger (1988). This catalogues 516 'infrared-excess' clouds, i.e., regions with anomalously high 100 μm to 21 cm line ratios. There are no such clouds close to the line of sight to NGC 55, implying $2N_{\rm H_2} < 4 \times 10^{19}$ cm^{-2}. To estimate the column of ionized hydrogen we first use the global electron density distribution of Reynolds (1991a). This has been derived from the dispersion measures ($\int n_{\rm e}\, dl$) of pulsars situated in globular clusters with known distances. Integrating the distribution along the line of sight of NGC 55 to a distance 4 kpc above the Galactic plane (the predicted maximum extent of the electron distribution) gives $N_{\rm e} = 7.4 \times 10^{19}$ cm^{-2}. Ideally, we could use nearby pulsars to obtain more local measurements; however, the nearest pulsars which could be used are $\sim 21°$ distant, ruling out this approach. For a sample of four pulsars Reynolds (1991b) has used the dispersion and emission measures ($\int n_{\rm e}^2\, dl$ as measured from the interstellar Hα intensity) to constrain the density and filling fraction of ionized hydrogen. This work implies that towards NGC 55 $N_{\rm e} = (4.1–7.7) \times 10^{19}$ cm^{-2}, in general agreement with the results quoted above. This estimate of the electron column density is essentially the same as that deduced by BW94 in the case of NGC 4725/4747. As noted by BW94, any neutral or partially ionized helium associated with this ionized component of the ISM will add to the effective line-of-sight column density at the rate $\Delta N_{\rm gal} \sim (0.4–0.65) \times N_{\rm e}$. Thus, as in BW94, we have recalculated the extragalactic intensity at 0.25 keV after increasing the Galactic $N_{\rm H}$ by 3×10^{19} and 5×10^{19} cm^{-2} (representative of a reasonable range of ionization states for the additional helium component). The weighted mean estimates of $C_{\rm ext}$ for these revised foreground column densities are listed in Table 4. Since the uncertainty in the Galactic H I column

[2] In calculating the relevant transmission factors from measured H I column densities we assume that the gas is cold (i.e., neutral) and can be characterized by the abundances and photoelectric absorption cross-sections tabulated by Morrison & McCammon (1983).

© Royal Astronomical Society • Provided by the NASA Astrophysics Data System

1996MNRAS.282..157B

derived from the Stark et al. (1992) measurements is $\sim 10^{19}$ cm^{-2}, we also quote the result for the lower limit $N_H = 1.45 \times 10^{20}$ cm^{-2}.

5 DISCUSSION

Prior to *ROSAT*, the best estimate of the intensity of the *total* extragalactic XRB at 0.25 keV had been obtained from wide-beam measurements of the shadowing of the soft XRB by neutral gas in the SMC (McCammon et al. 1976). McCammon & Sanders (1990) quote an up-dated result from this study, namely that the 95 per cent confidence upper limit for flux originating from beyond the SMC is 30 keV cm^{-2} s^{-1} sr^{-1} keV^{-1}. McCammon & Sanders (1990) also point out that their upper limit will need to be revised upperwards by a significant factor (i.e., ~ 1.5) if there is substantial additional soft X-ray opacity in our Galaxy due to He I and/or He II associated with the ionized component of the ISM. Of course, this important caveat also applies to other shadowing studies, including the present work (see Section 4).

More recently, a number of shadowing studies have been reported which make full use of the high spatial resolution of the *ROSAT* telescope and the low intrinsic background of the *ROSAT* PSPC. BW94 obtained a 95 per cent upper limit of 40 keV cm^{-2} s^{-1} sr^{-1} keV^{-1} based on a search for shadow cast by the H I associated with the galaxy pair NGC 4725/4747. Snowden & Pietsch (1995) in their analysis of the *ROSAT* observations of M101 note a depression in the 0.25-keV surface brightness which correlates with a galactic spiral arm, and from which they derive an estimate of the extragalactic XRB intensity at 0.25 keV of 28 ± 10 keV cm^{-2} s^{-1} sr^{-1} keV^{-1}. Also, Cui et al. (1996) quote a 95 per cent *lower limit* of 28 ± 10 keV cm^{-2} s^{-1} sr^{-1} keV^{-1} based on an analysis of the properties of a sample of face-on galaxies. In the present paper we detect the shadow cast by the outer H I disc of NGC 55, and use this to determine the intensity of extragalactic XRB at 0.25 keV to be 29.4 ± 7.2 keV cm^{-2} s^{-1} sr^{-1} keV^{-1}. Thus there is evidence for a convergence of recent measurements.

The spectrum of the extragalactic XRB in the soft X-ray band can, in principle, be obtained by combining our present measurements at 0.25 keV with recent estimates of the normalization of the extragalactic spectrum at 1 keV. Since shadowing measurements are not practical at this higher energy, these latter estimates rely on spectral modelling of data drawn typically from the 0.5–2 keV band with multiple (i.e., Galactic and extragalactic) components. Using *ROSAT* data, Hasinger et al. (1993) quote a value for the total extragalactic background flux in the 1–2 keV band of 1.25×10^{-8} erg cm^{-2} s^{-1} sr^{-1}. The corresponding 1-keV normalization ranges from 9.1 to 11.3 keV cm^{-2} s^{-1} sr^{-1} keV^{-1} if the underlying spectral form is a power-law continuum with α in the range 0.4–1.0. Analysis of *ROSAT* data has variously suggested the steeper ($\alpha = 1$) (Hasinger 1992; BW94) and the flatter ($\alpha = 0.4$–0.7) forms (Shanks et al. 1991; Wang & McCray 1993; Georgantopoulos et al. 1996). More recently, Gendreau et al. (1995) from an analysis of *ASCA* observations have argued that a single hard power law with $\alpha \approx 0.4$ provides a good description of the full 1–10 keV spectrum, with no evidence for a steepening in the 1–3 keV range. These authors determine values for the 1-keV normalization in the range 8.6–10.2 keV cm^{-2} s^{-1} sr^{-1} keV^{-1}, which is not far removed from the value of 7.7 keV cm^{-2} s^{-1} sr^{-1} keV^{-1} obtained as a power-law extrapolation of the 3–10 keV spectrum measured by *HEAO-1* (Marshall et al. 1980). There is thus some uncertainty as to the exact intensity and spectral slope of the extragalactic XRB at 1 keV; for the present purpose we make the conservative assumption that the relevant 1-keV normalization is 10 ± 1.5 keV cm^{-2} s^{-1} sr^{-1} keV^{-1}.

If we combine our present 0.25-keV measurement with the 1-keV estimate noted above, we obtain an effective spectral slope for the extragalactic XRB in the 0.25–1.0 keV energy range of $\alpha = 0.8 \pm 0.3$. However, a significant fraction of the 1-keV XRB has been resolved into discrete sources which appear to have rather steep intrinsic spectra. For example, Hasinger et al. (1993) estimate that 59 per cent of the 1–2 keV background is resolved in the deepest available *ROSAT* observations (which reach a 0.5–2.0 keV flux level of 2.5×10^{-15} erg cm^{-2} s^{-1}), and find that the combined source spectrum has a power-law slope of $\alpha \approx 1.0$ with little or no evidence for absorption intrinsic to the sources. The bulk of the discrete sources at somewhat higher flux thresholds appear to be QSOs (e.g. Shanks et al. 1991). Boyle et al. (1994) have studied the X-ray luminosity function and evolution exhibited by this source population and find that QSOs contribute between 0.34 and 0.53 of the 1–2 keV XRB, depending on the assumed evolutionary model. If we make the conservative assumption that as little as ~ 35 per cent of the extragalactic XRB signal at 1 keV has been resolved by *ROSAT* into QSOs with typical spectra slopes of

Table 4. Upper and lower bounds to the 0.25-keV XRB intensity.

Assumed N_H (10^{20} cm^{-2})	C_{ext} (count s^{-1} $arcmin^{-2}$)	Total 0.25 keV XRB intensity (keV cm^{-2} s^{-1} sr^{-1} keV^{-1})
1.55	$228 \pm 90 \times 10^{-6}$	29.4 ± 7.2
upper limits		
1.85	$273 \pm 113 \times 10^{-6}$	33.0 ± 9.0
2.05	$307 \pm 128 \times 10^{-6}$	35.7 ± 10.2
lower limit		
1.45	$216 \pm 87 \times 10^{-6}$	28.5 ± 6.7

© Royal Astronomical Society • Provided by the NASA Astrophysics Data System

1996MNRAS.282..157B

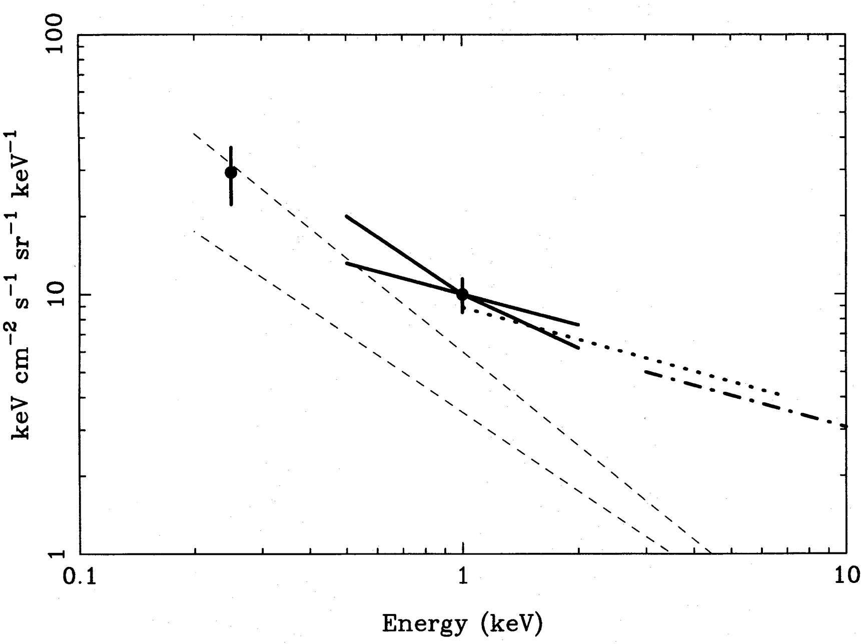

Figure 5. A schematic of the spectral form of the extragalactic XRB in the 0.1–10 keV band. The measurement at 0.25 keV is from the present work. The value of the normalization at 1 keV is shown as 10 ± 1.5 keV cm^{-2} s^{-1} sr^{-1} keV^{-1}. The solid lines show likely constraints on the slope of the XRB near 1 keV as derived from recent *ROSAT* observations. The hard power-law forms extending above 2 keV represent the *ASCA* (dotted line) and *HEAO-1* (dash-dotted line) measurements. The estimated minimum and maximum contributions of the integrated emission from QSOs are also indicated (dashed lines).

$\alpha = 1$ (and no measurable intrinsic absorption within the 0.1–0.4 keV band), then the residual extragalactic XRB spectrum from 0.25 to 1 keV has a spectral index $\alpha \approx 0.6$. At the other extreme, if the resolved fraction is ~ 60 per cent and QSO spectra are more typically characterized by $\alpha \approx 1.2$, then we have already accounted for the whole of the 0.25-keV extragalactic XRB. Fig. 5 provides a schematic summary of the available constraints on the spectral form of the extragalactic XRB and the integrated QSO contribution as noted above.

6 CONCLUSIONS

We have used *ROSAT* observations of the shadow cast by the disc of the nearby spiral galaxy NGC 55 to derive a new measurement of the total extragalactic background signal at 0.25 keV. We obtain 29.4 ± 7.2 keV cm^{-2} s^{-1} sr^{-1} keV^{-1} for the extragalactic XRB intensity at 0.25 keV, which is in excellent agreement with earlier constraints and estimates of this quantity. The spectrum of the extragalactic XRB in the soft X-ray (0.25–1 keV) band is now fairly well constrained, some 15 years after the definitive *HEAO-1* measurements covering the 3–50 keV energy range were published. It is somewhat perverse that the most recent part of the XRB spectrum to be measured may turn out to be the first to be fully explained in terms of the integrated emission of *known* populations of sources.

ACKNOWLEDGMENTS

We thank Steve Snowden for providing software relating to the *ROSAT* PSPC background and detector efficiency map. CRB and TPR acknowledge financial support from PPARC. The *ROSAT* data used in this project were obtained from the Leicester Database and Archive Service (LEDAS).

REFERENCES

Allen D. J., 1992, ASTERIX User Note 004
Barber C. R., Warwick R. S., 1994, MNRAS, 267, 270 (BW94)
Boyle B. J., Shanks T., Georgantopoulos I., Stewart G. C., Griffiths R. E., 1994, MNRAS, 271, 639
Burrows D., Mendenhall J., 1991, Nat, 351, 629
Comastri A., Setti G., Zamorani G., Hasinger G., 1995, A&A, 296, 1
Cui W. et al., 1996, ApJ, submitted
Desert F. X., Bazell D., Boulanger F., 1988, ApJ, 334, 815
de Vaucouleurs G., de Vaucouleurs A., Corwin Jr, H. G., 1976, Second Reference Catalogue of Bright Galaxies. Univ. Texas, Austin
Fabian A., Barcons X., 1992, ARA&A, 30, 429
Gendreau K. C. et al., 1995, PASJ, 47, L5
Georgantopoulos I., Stewart G. C., Shanks T., Boyle B. J., Griffiths R. E., 1996, MNRAS, 280, 276
Giacconi R., Gursky H., Paolini F., Rossi B., 1962, Phys. Rev. Lett., 9, 439
Hasinger G., 1992, in Barcons X., Fabian A., eds, The X-ray Background. Cambridge Univ. Press, Cambridge, p. 229
Hasinger G., Burg R., Giacconi R., Hartner G., Schmidt M., Trumper J., Zamorani G., 1993, A&A, 275, 1
Hummel E., Dettmar R. J., Wielebinski R., 1986, A&A, 166, 97
Madau P., Ghisellini G., Fabian A., 1994, MNRAS, 270, L17
Marshall F. E., Boldt E. A., Holt S. S., Miller R. B., Mushotzky R. F., 1980, ApJ, 235, 4
McCammon D., Sanders W. T., 1990, ARA&A, 28, 657
McCammon D., Meyer S. S., Sanders W. T., Williamson F. O., 1976, ApJ, 209, 46

© Royal Astronomical Society • Provided by the NASA Astrophysics Data System

1996MNRAS.282..157B

Morrison R., McCammon D., 1983, ApJ, 270, 119
Nousek J., Fried P., Sanders W., Kraushaar W., 1982, ApJ, 258, 83
Plucinsky P., Snowden S., Briel U., Hasinger G., Pfeffermann E., 1993, ApJ, 418, 519
Puche D., Carignan C., 1988, ApJ, 95, 1025
Puche D., Carignan C., Wainscoat R. J., 1991, AJ, 101, 447
Reynolds R., 1991a, in Bloemen H., ed., The Interstellar Disk–Halo Connection in Galaxies. Kluwer, Dordrecht, p. 67
Reynolds R., 1991b, ApJ, 372, L17
Schmitt J. H. M. M., Snowden S. L., 1990, ApJ, 361, 207
Shanks T., Georgantopoulos I., Stewart G. S., Pounds K. A., Boyle B., Griffiths R. E., 1991, Nat, 353, 315
Snowden S. L., Pietsch W., 1995, ApJ, 452, 627
Snowden S., Cox D., McCammon D., Sanders W., 1990, ApJ, 354, 211
Snowden S., Mebold U., Hirth W., Herbstmeier U., Schmitt J. H. M. M., 1991, Science, 252, 1529
Snowden S., Plucinsky P., Briel U., Pfeffermann G. H. E., 1992, ApJ, 393, 819
Snowden S. L., McCammon D., Burrows D. N., Mendenhall J. A., 1994, ApJ, 424, 714
Stark A. A., Gammie C. F., Wilson R. W., Bally J., Linke R. A., Heiles C., Hurwitz M., 1992, ApJS, 79, 77
Tully R. B., 1988, Nearby Galaxies Catalog, Cambridge Univ. Press, Cambridge
Wang Q. D., McCray R., 1993, ApJ, 409, L37
Wang Q. D., Yu K. C., 1995, AJ, 109, 698

APPENDIX A: SHADOWING MEASUREMENTS – THE EFFECT OF A VARYING SOURCE EXCLUSION THRESHOLD

In BW94 the 0.25-keV extragalactic XRB intensity was calculated for each pixel in the shadowed region via the expression

$$C_{\rm ext} = \frac{\bar{C} - C_{{\rm obs},i}}{T_{\rm gal} - T_{{\rm tot},i}}. \tag{A1}$$

Here $C_{\rm ext}$ is the value of the 0.25-keV extragalactic XRB intensity, fully corrected for absorption, as derived from the count rate $C_{{\rm obs},i}$ measured in the ith pixel. $\bar{C}$ is the mean intensity in the control sample, $T_{\rm gal}$ is the transmission factor for an extragalactic signal in the control region (based solely on the foreground Galactic H I column density), and $T_{{\rm tot},i}$ is the equivalent transmission factor for the ith pixel (including the absorption in the H I disc of the shadowing galaxy).

An error was assigned to each measurement, assuming that the $C_{{\rm obs},i}$ values originate from a Gaussian distribution with the same standard deviation as the control sample. The weighted mean of the $C_{\rm ext}$ values over the set of 'on-source' pixels is then taken as the best estimate of the extragalactic XRB intensity.

This approach must be modified in the situation where the flux threshold for the exclusion of bright discrete sources varies due to the additional absorption in the shadowing target. The average intensity measured in the control region can be equated to the sum of the local foreground emission ($C_{\rm for}$) plus the transmitted fraction of the *unresolved* extragalactic signal:

$$\bar{C} = C_{\rm for} + T_{\rm gal} C_{\rm ext} \tag{A2}$$

The equivalent expression for a pixel in the shadowed region is

$$C_{{\rm obs},i} = C_{\rm for} + T_{{\rm tot},i}(C_{\rm ext} + \Delta C_{{\rm ext},i}). \tag{A3}$$

The $\Delta C_{{\rm ext},i}$ term reflects the fact that the intensity of the *unresolved* extragalactic XRB is somewhat higher for a pixel in the shadowed region since $T_{{\rm tot},i} < T_{\rm gal}$, and thus there is a higher source exclusion threshold in terms of *intrinsic* source flux. Note that if we set $\Delta C_{{\rm ext},i} = 0$, then the elimination of $C_{\rm for}$ from equations (A2) and (A3) takes us back to equation (A1).

The correct expression for $C_{\rm ext}$ is then

$$C_{\rm ext} = \frac{\bar{C} - C_{{\rm obs},i}}{T_{\rm gal} - T_{{\rm tot},i}} + \frac{\Delta C_{{\rm ext},i} T_{{\rm tot},i}}{T_{\rm gal} - T_{{\rm tot},i}}. \tag{A4}$$

In practice, the values of $\Delta C_{{\rm ext},i}$ are calculated as:

$$\Delta C_{{\rm ext},i} = AF \int_{S_{\rm low}}^{S_{\rm high}} N(S) S \, {\rm d}S, \tag{A5}$$

where $N(S)$ is the differential form of the 0.5–2.0 keV source counts (e.g. Hasinger et al. 1993), F is the conversion factor from a 0.5–2.0 keV band flux (S) to a 0.25-keV band count rate (C) (assuming a particular continuum form but no absorption), and A represents the relevant solid angle conversions. The limits of the integration are $S_{\rm high} = C_{\rm min}/FT_{{\rm tot},i}$ and $S_{\rm low} = C_{\rm min}/FT_{\rm gal}$, where $C_{\rm min}$ is the 0.25-keV source detection threshold.

© Royal Astronomical Society • Provided by the NASA Astrophysics Data System